EARTHQUAKE ENGINEERING AND STRUCTURAL DYNAMICS
Earthquake Engng Struct. Dyn. 2006; **35**:1767–1785
Published online 6 July 2006 in Wiley InterScience (www.interscience.wiley.com). DOI: 10.1002/eqe.603

Shaking table tests on seismic response of steel braced frames with column uplift

Mitsumasa Midorikawa[1,*,†], Tatsuya Azuhata[2], Tadashi Ishihara[2] and Akira Wada[3]

[1]*Graduate School of Engineering, Division of Architectural and Structural Design, Hokkaido University, Kita 13, Nishi 8, Kita-ku, Sapporo 060-8628, Japan*
[2]*National Institute for Land and Infrastructure Management, Ministry of Land, Infrastructure and Transport, 1 Tachihara, Tsukuba, Ibaraki 305-0802, Japan*
[3]*Structural Engineering Research Center, Tokyo Institute of Technology, 4259 Nagatsuta, Midori-ku, Yokohama, Kanagawa 226-8503, Japan*

SUMMARY

Previous studies have suggested that rocking vibration accompanied by uplift motion might reduce the seismic damage to buildings subjected to severe earthquake motions. This paper reports on the use of shaking table tests and numerical analyses to evaluate and compare the seismic response of base-plate-yielding rocking systems with columns allowed to uplift with that of fixed-base systems. The study is performed using half-scale three-storey, 1×2 bay braced steel frames with a total height of 5.3 m. Base plates that yield due to column tension were installed at the base of each column. Two types of base plates with different thicknesses are investigated. The earthquake ground motion used for the tests and analyses is the record of the 1940 El Centro NS component with the time scale shortened by a factor of $1/\sqrt{2}$. The maximum input acceleration is scaled to examine the structural response at various earthquake intensities. The column base shears in the rocking frames with column uplift are reduced by up to 52% as compared to the fixed-base frames. Conversely, the maximum roof displacements of the fixed and rocking frames are about the same. It is also noted that the effect of the vertical impact on the column associated with touchdown of the base plate is small because the difference in tensile and compressive forces is primarily due to the self-limiting tensile force in the column caused by yielding of the base plate. Copyright © 2006 John Wiley & Sons, Ltd.

Received 18 March 2005; Revised 25 December 2005; Accepted 10 May 2006

KEY WORDS: seismic response reduction; rocking vibration; steel frame; column uplift; yielding base plate

*Correspondence to: Mitsumasa Midorikawa, Graduate School of Engineering, Division of Architectural and Structural Design, Hokkaido University, Kita 13, Nishi 8, Kita-ku, Sapporo 060-8628, Japan.
†E-mail: midorim@eng.hokudai.ac.jp

Contract/grant sponsor: Ministry of Education, Culture, Sports, Science and Technology of Japan; contract/grant numbers: 16360284, 16560520

1. INTRODUCTION

Past studies have pointed out that the effects of rocking vibration accompanied with uplift motion may reduce the seismic damage to buildings subjected to strong earthquake ground motions [1, 2]. Based on these studies, structural systems have been developed that permit rocking vibration and uplift motion under appropriate control during major earthquake ground motions [3–7]. When rocking structural systems are applied to building structures, some advantages are expected in the seismic design of buildings. As shown in Figure 1, these systems can lead to reduced seismic response, which might lead to a more rational and economical seismic design of not only superstructures, but also foundations.

Up to a certain point, the influence of uplift motion on the seismic behaviour of buildings can be explained through simple analyses [8]. Studies have demonstrated that the maximum strain energy associated with the horizontal deformation of a structure is reduced in rocking structural systems because a portion of the total seismic energy applied to a structure is dissipated by the potential and kinetic energy associated with vertical motion [9]. However, further study is required to examine several issues such as the increase in the horizontal displacement response and the effects of column base impact associated with rocking. Although studies have pointed out that the installation of dampers in the uplift portion is effective in reducing the horizontal displacement response of a structure, details of such effects have not been discussed [6, 7].

A rocking structural system under development by the authors employs the yielding mechanism of base plates. When weak base plates yield due to column tension during a strong earthquake ground motion, the columns uplift and enable the building structure to rock. The basic concept of the base-plate-yielding system is illustrated in Figure 2. In this system, the yielding base plates dissipate some of the input seismic energy by their inelastic behaviour.

In this paper, shaking table tests and numerical analyses are used to evaluate and compare the seismic response of base-plate-yielding rocking structural systems with column uplift with that of

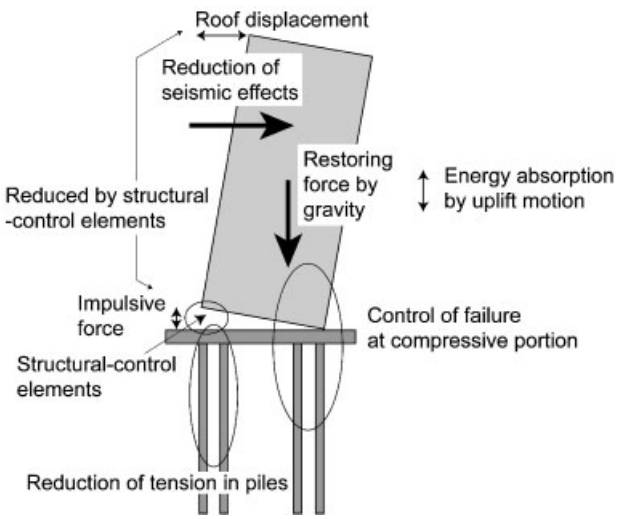

Figure 1. Structural rocking systems.

DOI: 10.1002/eqe

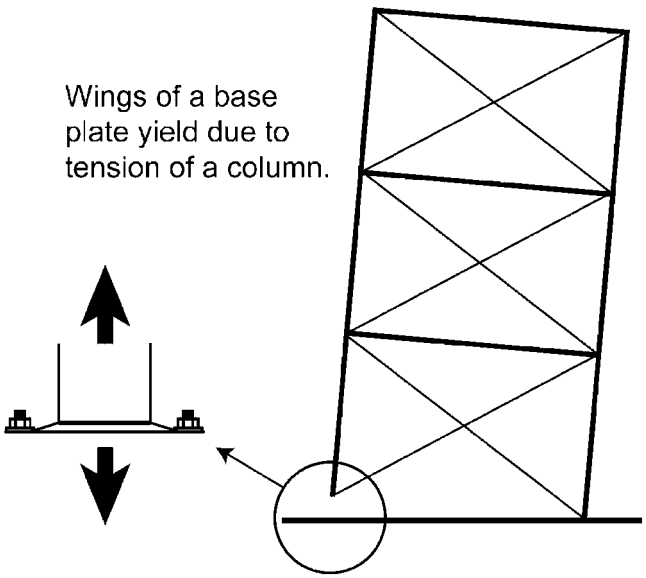

Figure 2. Structural rocking systems with yielding base plates.

fixed-base systems. The objectives of the study are to improve the understanding of the dynamic rocking response of structures subjected to earthquake motions, to demonstrate the feasibility of designing steel frames to enable the rocking response through column base-plate deformations, and to validate analytical models to simulate the response of rocking through column uplift. The test frames in this study are intended to provide the means for evaluating the base plate behaviour and the rocking response in steel buildings, but they do not necessarily represent the actual conditions of real buildings.

When base-plate-yielding systems are applied to actual buildings, the configuration and the mechanical characteristics of the base plates, such as their uplift yield strength, must first be determined. Therefore, we need to study the relationship between the mechanical characteristics of the yielding base plates and the critical base shear of the uplift response. A simplified analytical method is proposed to grasp this relationship and to predict the fundamental characteristics of the seismic responses of these systems. The applicability of this analytical method is discussed and verified in References [10, 11] that consider the energy balance of a system to predict the maximum response displacements including uplift.

2. TEST STRUCTURES AND EXPERIMENTAL PROCEDURES

Three-storey half-scale braced steel frames were tested on the shaking table at the National Research Institute for Earth Science and Disaster Prevention in Tsukuba, Japan. The test frames were retested using four different base conditions (F, BP6, BP9, and BP9-2). The test structures are composed of yielding base plates, columns, girders, and bracing members, as shown in Figures 3 and 4. There is no significant difference between the central frame and the end frames. The total height of the

DOI: 10.1002/eqe

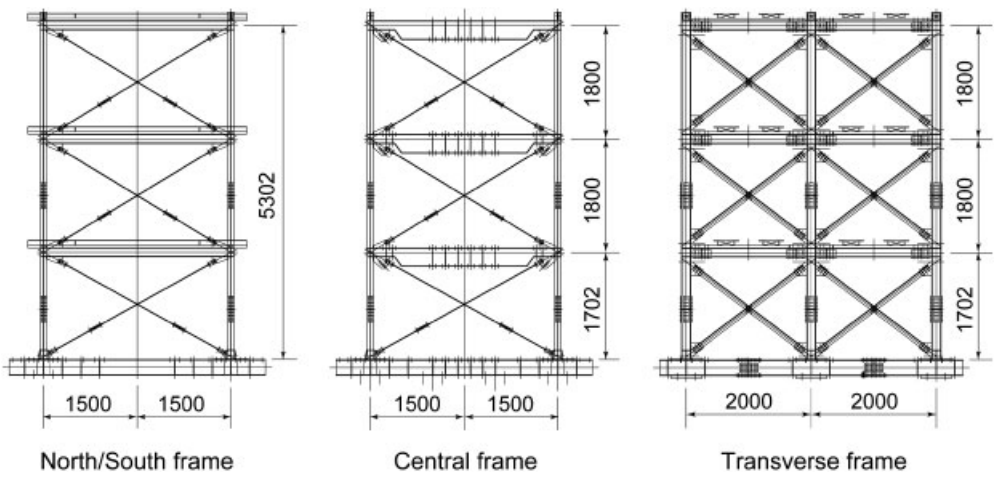

Figure 3. Elevation of test structure.

Figure 4. General view of test structure.

Table I. Floor weight.

Floor	Weight (kN)
Roof	45
3	51
2	51

test structures is 5.3 m, 1.7 m for the first storey and 1.8 m each for the second and third stories. The floor dimension is 3×4 m and the total weight of the structure is 147 kN. The weight of each floor and the member cross-section properties are summarized in Tables I and II, respectively.

DOI: 10.1002/eqe

Table II. Cross sections of members.

Member	Size (mm)
Column	H-148 × 100 × 6 × 9
Girder	H-150 × 150 × 7 × 10*
	H-300 × 150 × 6.5 × 9†
	(H-150 × 150 × 6.5 × 9‡)
Brace	ϕ-11

*North/South frame.
†Middle part of a girder of central frame.
‡End part of a girder of central frame.

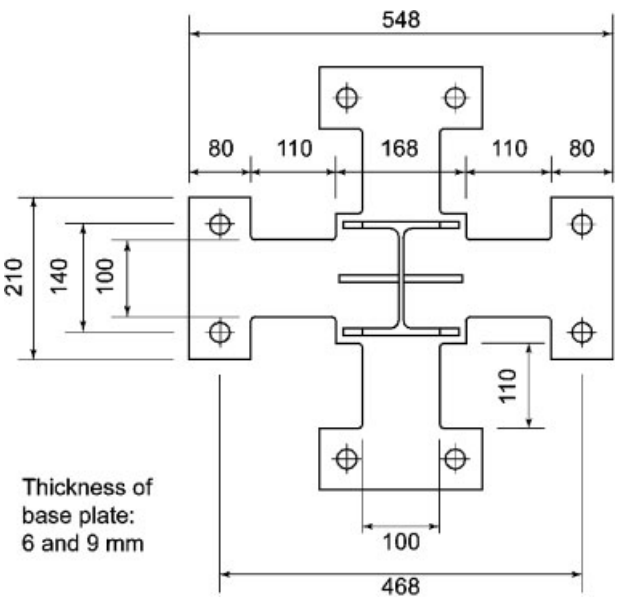

Figure 5. Plan of yielding base plate.

In the shaking direction, the test structure has three braced frames with a span of 3 m each. The bracing member is a high-strength prestressed steel bar with a diameter of 11 mm and tensile strength of 980 MPa. These bracing members are prestressed to the tension strain of 0.1% so that they resist both compression and tension forces. In the transverse direction, the test structure is braced by diagonal bracing members of angle steel of L-75 × 12 bolted to the frames.

Yielding base plates are installed at the bottom of each column of the first storey of the test structures, as shown in Figures 5 and 6. Two types of base plates with different thicknesses of 6 and 9 mm are used in the tests. The mechanical characteristics of the base plates are listed in Table III. The test structures with base plate thicknesses of 6 or 9 mm are referred to as BP6 and BP9 models, respectively, and the test structure with a fixed base in the conventional fixed-base support condition is referred to as F model. The base plates of BP6 and BP9 models have four

DOI: 10.1002/eqe

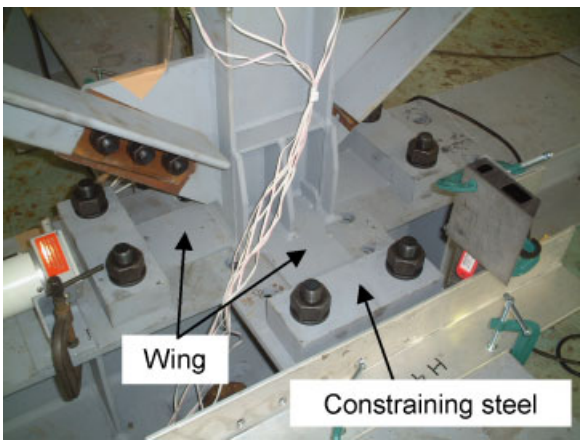

Figure 6. Close-up of yielding base plate.

Table III. Mechanical characteristics of yielding-base-plate steel.

Model	JIS*	Yield strength (MPa)
BP6	SS400	330
BP9	SS400	292

*JIS: Japanese Industrial Standard.

Table IV. Characteristic values of yielding base plates.

Model	BP6	BP9	BP9-2
Uplift yield strength (kN)	23.8	47.3	23.7
Uplift yield displacement (mm)	1.3	0.79	0.79

wings that are each 110 mm long and 100 mm wide. The test structure with the base plates of two wings 9-mm thick along the shaking direction, is referred to as BP9-2 model. The outside end of each wing of each base plate is constrained and connected to a steel foundation beam by a steel plate 40 mm thick and two high-strength bolts so that plastic hinge lines are formed at both ends of each wing. The characteristic values of each yielding base plate are listed in Table IV. The uplift yield strength of the base plate is based on the estimated value and conditions of the following: (a) the response acceleration at the instant when uplifting starts that is estimated based on the overturning moment of the superstructure including the uplift yield strength of the base plate, (b) that the uplift yield strength of the base plate should not exceed the axial dead load of a column so that the dead load compression is enough to overcome any residual deformations in the base plate, and (c) that only the base plate wings subjected to in-plane tensile force should resist the shear transmitted from the superstructure without consideration of the base plate wings at the uplifting columns.

DOI: 10.1002/eqe

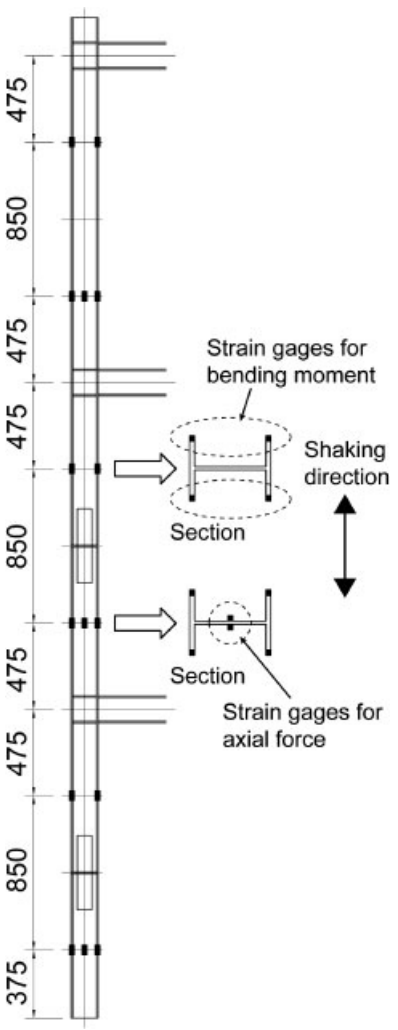

Figure 7. Locations of strain gauges attached to columns.

The test structures are vibrated in a horizontal direction, which coincides with the strong axis of each column such that the columns are subjected to bending about the weak axis. The earthquake ground motion used for the tests is the NS component of the 1940 El Centro record with its time scale shortened to $1/\sqrt{2}$, resulting in a duration of 24 s. Each test structure is subjected to earthquake ground motions several times with the maximum input acceleration scaled to a range of levels to simulate various earthquake intensities.

The instrumentation was designed to measure both global structural response and local element response in critical portions of the test frames. The measured data include the following: horizontal accelerations on the shaking table, horizontal accelerations and relative horizontal displacements at each floor level, axial strains of the columns and bracing members, and uplift displacements of

DOI: 10.1002/eqe

the first storey column bases. The maximum sampling frequency is 2000 Hz. The column shears are calculated from the moment distribution using measured values of strain gauges attached to columns as shown in Figure 7. The base shear is calculated by summing the shears of the columns and bracing members at the first storey. This value corresponds quite well with the base shear obtained from the measured accelerations and masses on each floor.

3. ANALYTICAL MODELLING AND NUMERICAL ANALYSES

Finite element analyses that were used to determine the seismic responses of the test frames were also investigated in ADINA report [12]. Figure 8 illustrates a mathematical idealization of the test structure. The base plates and the columns of the first storey are modelled using shell elements, as shown in Figure 8(b). The columns and girders at the second and third stories are modelled using beam elements, and the bracing members are modelled using truss elements (Figure 8(a)).

The base plate is modelled with an elastoplastic material considering finite deformations and a kinematic hardening rule with the Mises–Hencky yield condition. The other elements are assumed elastic. The initial tension strain of 0.1% is assumed in the bracing members that resist both tension and compression if tension does not disappear. In the shaking table tests, the bracing members were kept almost in tension. The steel foundation beam is assumed rigid. The contact conditions such as the normal contact force and the tangential contact slip without friction are considered between the rigid foundation beam and the shell elements of the base plates. A very small ramp-up region is defined in the base plate contact models.

The masses of the analytical model based on the actual dead loads of the test structure are lumped at each nodal point of the girders. The vertical components of the masses were defined in order to capture the effects of vertical inertia associated with rocking. The dead load corresponding to the lumped masses is applied to each node of the analytical model before starting the dynamic response analyses.

It is assumed that the viscous damping results from the initial stiffness-dependent effects. The critical damping ratio of 0.5%, that is the stiffness-proportional type, is introduced to the first mode

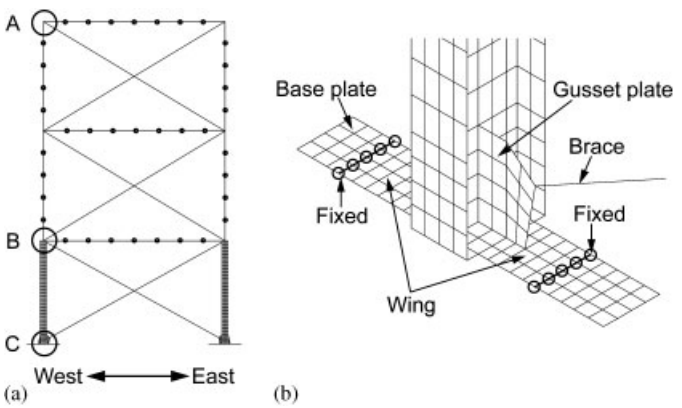

Figure 8. Finite element analytical model: (a) overall frame; and (b) details around base plates.

DOI: 10.1002/eqe

in bending corresponding to the fixed-base model whose value is compatible with the results from the shaking table tests on the test structures.

The numerical time integration in the analyses is the combined use of the Newmark method with constant acceleration and the Newton–Raphson method for equilibrium iteration with time steps of 0.001 s. The measured acceleration records from the shaking table tests are used as input for the dynamic response analyses. In the analyses, the duration is six seconds because the maximum response of the test structure was observed during this period.

4. TEST RESULTS AND DISCUSSION

4.1. Input motions and dynamic characteristics of the test structures

Figure 9 shows the acceleration response spectra for the El Centro ground motion record scaled by 0.5 and 1.75. The scaling of 1.75 results in a maximum input acceleration of 5.84 m/s^2. The motions reproduced by the shaking table have about the same frequency characteristics regardless of the intensity level of the input motions. Also shown in Figure 9 are the measured and calculated natural (1st mode) periods of the F and BP9-2 frames.

The fundamental natural period of F model obtained from the test using white noise input motion is 0.18 s and the critical damping ratio obtained from the bandwidth method is 0.5% for the first mode. The natural periods from the analytical results of BP9-2 model are 0.260 and 0.066 s for the first and second bending modes, respectively, while those of analytical F model are 0.160 and 0.056 s, respectively. The translational vibration mode shapes of the uplift analytical model in the first and second bending modes are illustrated in Figure 10, although the second-mode participation is not remarkable in the test results.

The response period of BP9-2 model subjected to the maximum input acceleration of 5.84 m/s^2 is up to about 0.34 s, as shown in Figure 11. Therefore, the range of the response periods of the test frames does not reach the region of constant velocity in the response spectra of input motions, as shown in Figure 9.

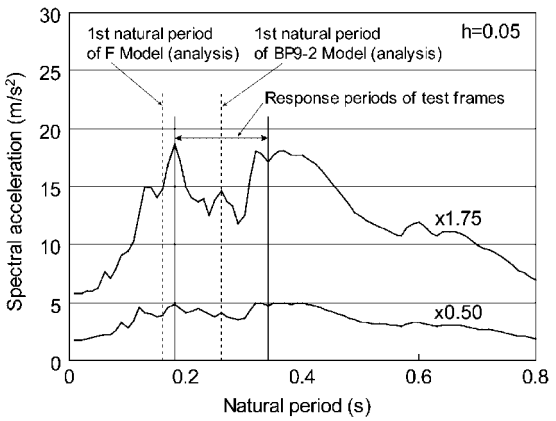

Figure 9. Acceleration response spectra of measured table accelerations.

DOI: 10.1002/eqe

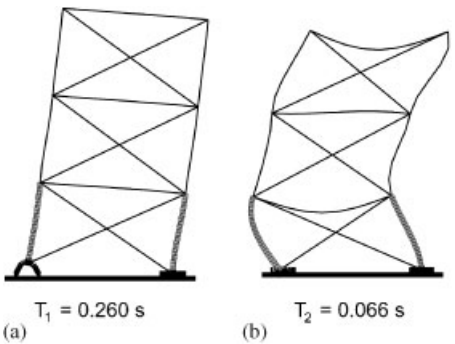

Figure 10. Translational vibration mode shapes in bending: (a) first bending mode; and (b) second bending mode.

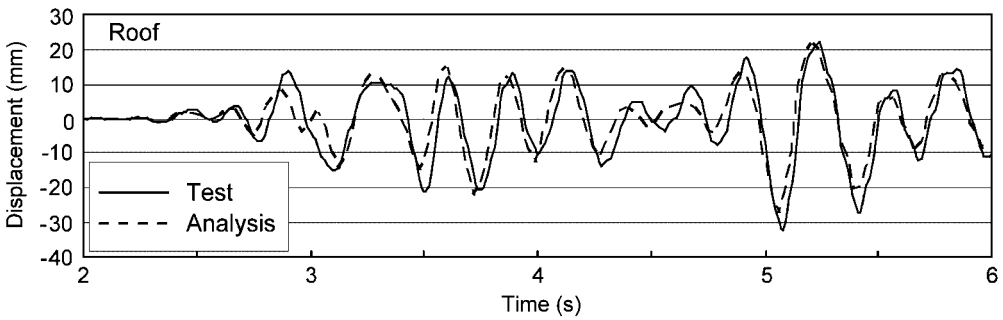

Figure 11. Time histories of roof displacement responses of BP9-2 model. Maximum input acceleration = 5.84 m/s^2.

4.2. Global behaviour and seismic response reduction effects

Figure 11 illustrates the time histories of the roof displacement responses of BP9-2 model. The test and analytical results are indicated by solid and broken lines, respectively. The test result is in good agreement with the analytical one. For the first bending mode of uplift analytical model, the translational vibration period is close to or slightly larger than the natural period of 0.26 s. The maximum roof displacement of 30.3 mm from the analytical result agrees approximately with that of 32.2 mm from the test result.

Figure 12 shows the relationships between the peak response values and input accelerations for each test structure. The dotted lines in Figures 12(b) and (c) indicate the extrapolated values from the test results of F model based on the assumption that the response of F model is elastic. With the exception of the base plates, not all the test structures were subjected to large ground motions in order to keep them elastic because the test structure was prepared as a multipurpose test bed. From the results of the shaking test measurements, it was concluded that the structural members remained elastic except for the base plates and that the central frame and the end frames of each test structure showed essentially identical behaviours.

DOI: 10.1002/eqe

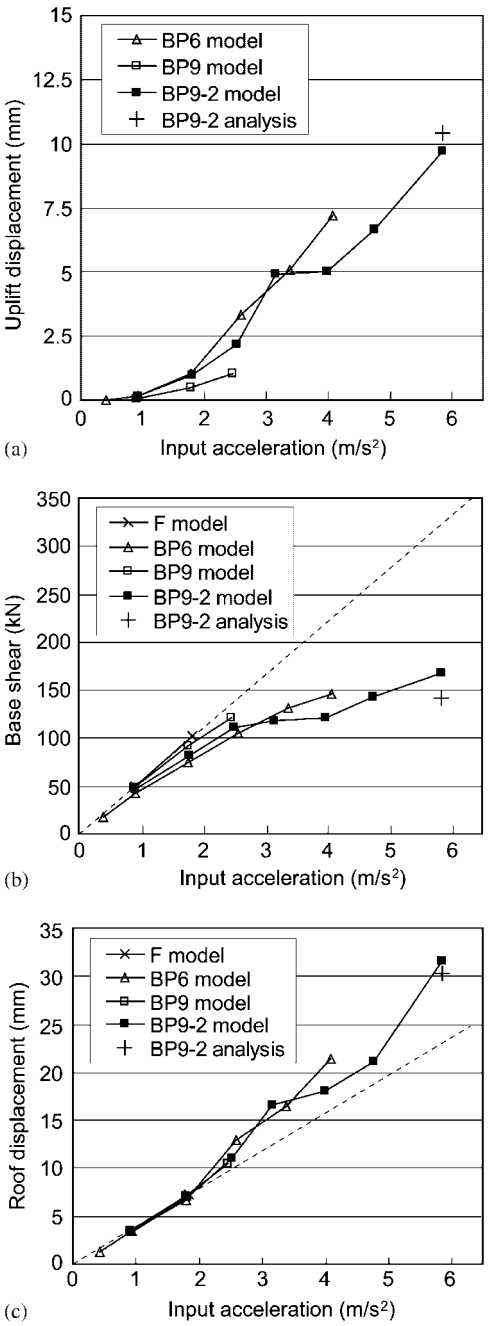

Figure 12. Maximum responses versus maximum input accelerations: (a) uplift; (b) base shear; and (c) roof displacement.

DOI: 10.1002/eqe

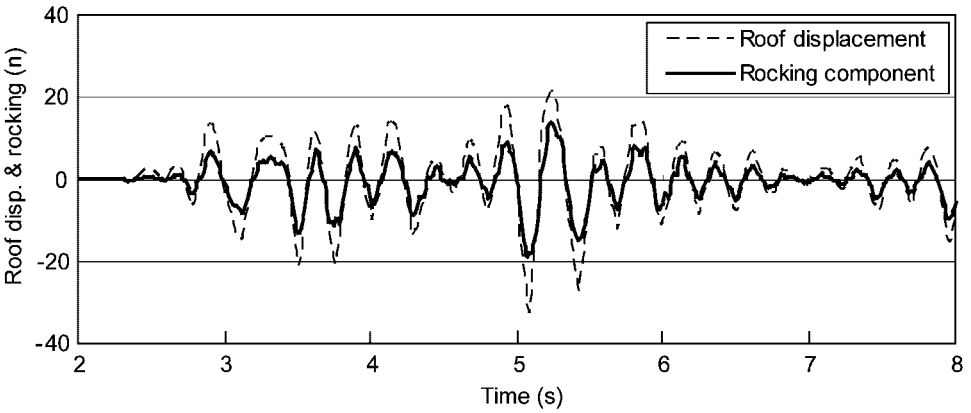

Figure 13. Time histories of roof displacement and rocking component of BP9-2 model. Maximum input acceleration = 5.84 m/s^2.

The uplift displacements are very small for maximum input accelerations up to about 2.0 m/s^2, as shown in Figure 12(a). As the input acceleration becomes larger, the uplift displacement increases monotonically. When the input acceleration becomes about 3.3 m/s^2, the uplift displacements of BP6 and BP9-2 models reach about 5 mm. In BP9-2 model, the uplift displacement attains 9.9 mm under an input acceleration of 5.84 m/s^2. The base shears of all test structures are almost the same when the maximum input acceleration is smaller than 2.0 m/s^2, as shown in Figure 12(b). When the input acceleration becomes larger than 2.5 m/s^2, the base shears resisted by BP6, BP9, and BP9-2 models are about 120 kN and the rate of increase becomes small. Furthermore, the base shears of BP6 and BP9-2 models are much smaller than were those of F model, as indicated by the dotted line in Figure 12(b). This indicates that the maximum base shears of the test structures with column uplift are effectively reduced from those of the fixed-base system, and that this reduction effect is remarkable in the case of systems with base plates having weaker uplift yield strength. The roof displacements of BP6, BP9, and BP9-2 models are all about the same as for F model, as shown in Figure 12(c). The analytical results of the maximum responses under the earthquake motion record scaled at 1.75 times for BP9-2 model are plotted using '+' marks in Figure 12. The analytical results correspond very well to the test results.

Figure 13 shows the time histories of the total roof displacement and the component of displacement due to rocking of BP9-2 model under the maximum input acceleration of 5.84 m/s^2. The rocking component contributes to about two-thirds of the roof displacement during the uplift motion. Figure 14 shows the maximum storey shear distribution along the height of the test frames. The storey shears of F model are extrapolated from the test results in Figure 14(b) based on the assumption that the response of F model is elastic as is observed in the test. When the maximum input acceleration is 0.9 m/s^2, the response values are almost the same among the test frames. When the input acceleration becomes 3.5 m/s^2, the seismic response reduction effect of the rocking structural systems is clearly observed and all storey shears of BP6 and BP9-2 models are smaller than were those of F model. From Figures 13 and 14, it is revealed that the response deformation of the superstructure is suppressed because the rocking component dominates the roof displacement.

DOI: 10.1002/eqe

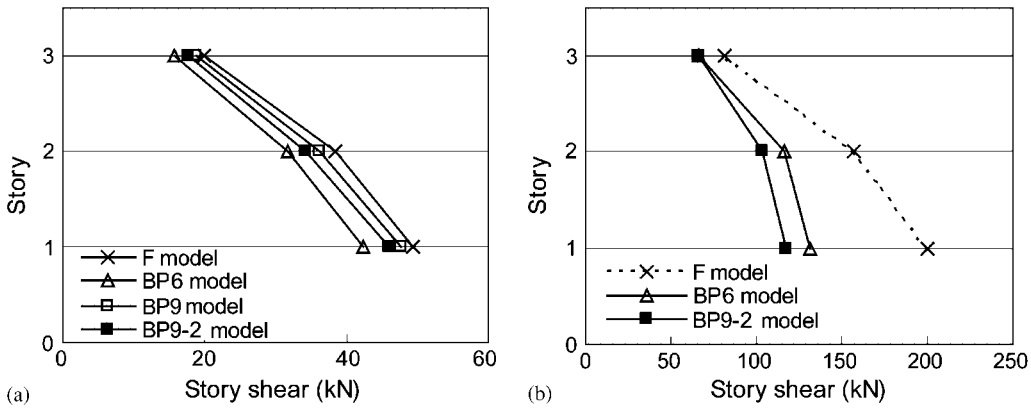

Figure 14. Maximum storey shears of test frames: maximum input acceleration = (a) 0.9 m/s^2; and (b) 3.5 m/s^2.

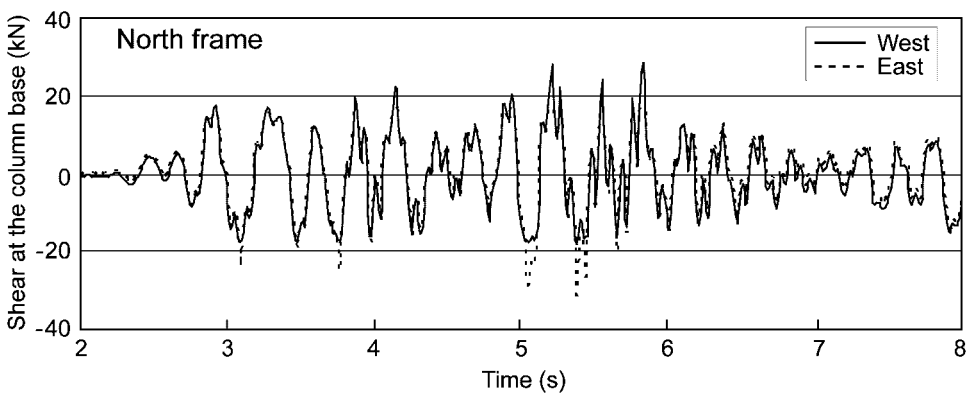

Figure 15. Time histories of shear forces at column bases of BP9-2 model. Maximum input acceleration = 5.84 m/s^2.

Figure 15 shows the time histories of the shear forces at the column bases of the north frame of BP9-2 model under the maximum input acceleration of 5.84 m/s^2. The shear force from west to east is positive, as is shown in Figure 16. The shear force at the column base is calculated by summing the shears from a column and a brace based on the measured strains. In Figure 15, the east column base suddenly resists more shear than does the west column base between 5 and 6 s. This resistance is attributed to the loss of tension in a bracing member. The shear force is effectively transmitted through the base plate while uplift is occurring. It should be noted that the uplift does not depreciate the shear transfer capacity of the base plate in the horizontal direction.

DOI: 10.1002/eqe

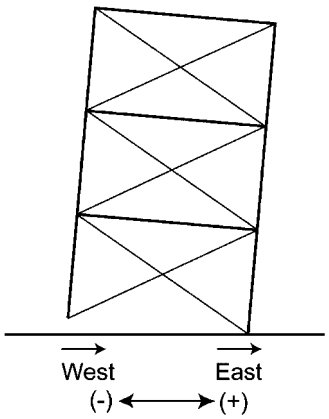

Figure 16. Shear forces at bottom of frame.

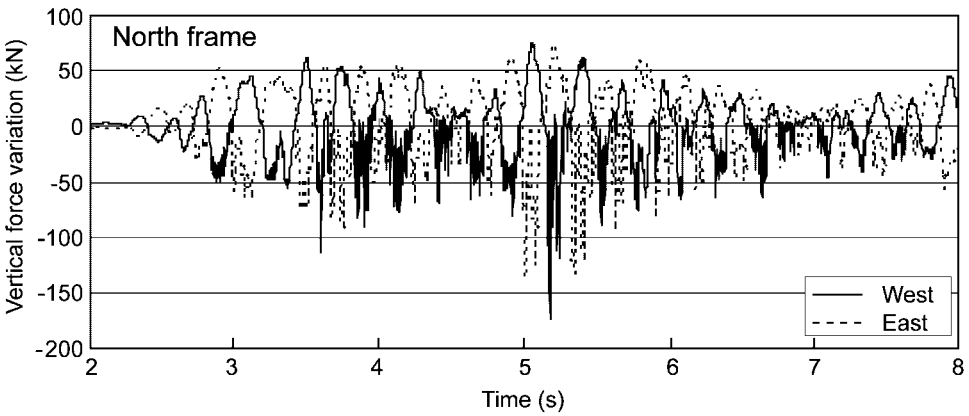

Figure 17. Time histories of vertical force variations at column bases of BP9-2 model. Maximum input acceleration = 5.84 m/s^2.

4.3. Uplift and vertical responses at the column bases

Figure 17 shows the time histories of the variations of vertical force at the column bases of the north frame of BP9-2 model under the maximum input acceleration of 5.84 m/s^2. The column axial forces are calculated from the measured data of strain gauges attached to the columns, as shown in Figure 7. Corresponding to this figure, the time histories of the uplift displacement responses of the central frame of BP9-2 model are illustrated in Figure 18. The peak uplift displacement reaches 9.9 mm, which corresponds to a rigid body rotation angle of 1/300 in the superstructure.

Figure 19 shows the relationships of the maximum vertical forces at the column bases and the maximum input accelerations for all models. In this figure, the vertical force includes the dead load effects. The variable range of the vertical forces is symmetrical in tension and compression before the uplift motion is induced. The tensile forces for the uplifting cases are limited to about

DOI: 10.1002/eqe

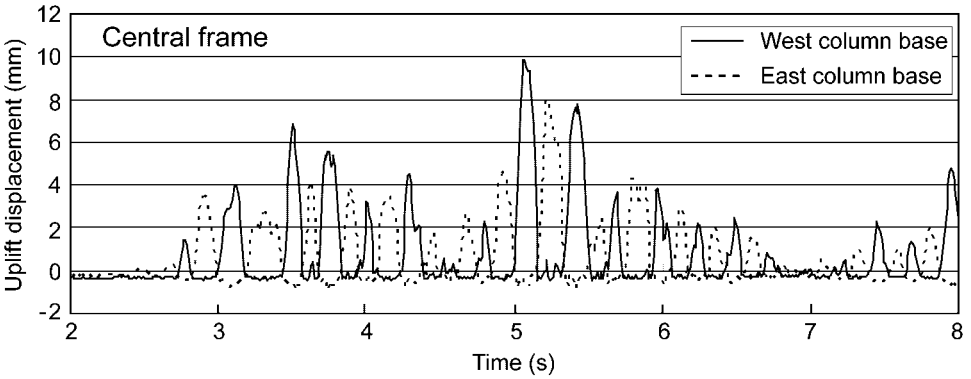

Figure 18. Time histories of uplift displacement responses of BP9-2 model. Maximum input acceleration = 5.84 m/s^2.

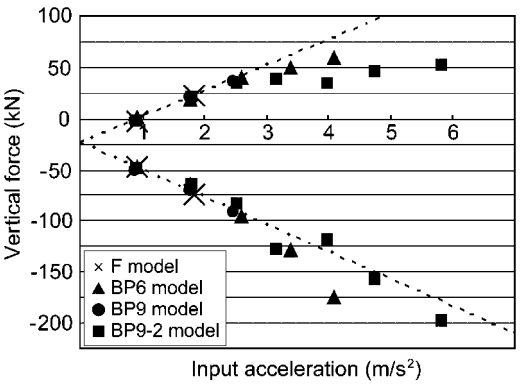

Figure 19. Maximum vertical forces versus maximum input accelerations.

twice of the uplift yield strength of the base plates after the uplift motion occurs. The increase in the tensile strength is caused by the inelastic strain hardening and large deformation effects in the wings of the base plates. The compressive forces for the uplifting cases are about the same as for the fixed base, as indicated by the dotted line in Figure 19. The impact effect is small because the difference in tensile and compressive forces is primarily due to the self-limiting tensile force in the column due to base plate yielding.

5. ANALYTICAL RESULTS AND DISCUSSION

5.1. Uplift behaviour and responses

The time histories of the uplift displacement responses at the centre of the base plate on the west side of BP9-2 model are shown in Figure 20 where the measured uplift displacement of the central

DOI: 10.1002/eqe

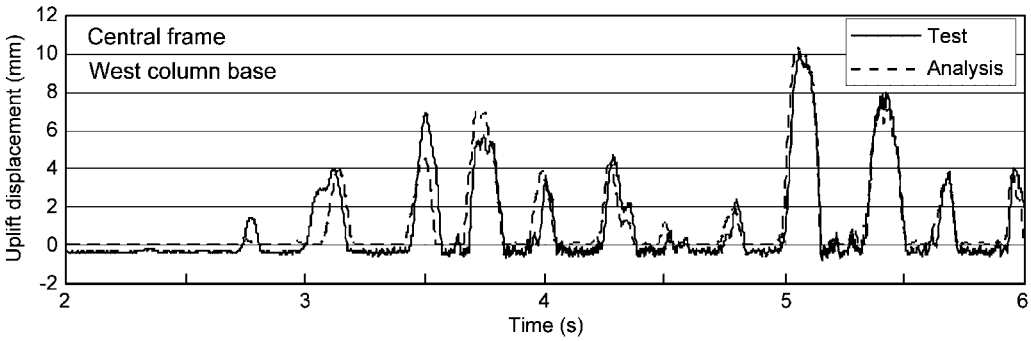

Figure 20. Time histories of uplift displacement responses at column base of BP9-2 model. Maximum input acceleration = 5.84 m/s^2.

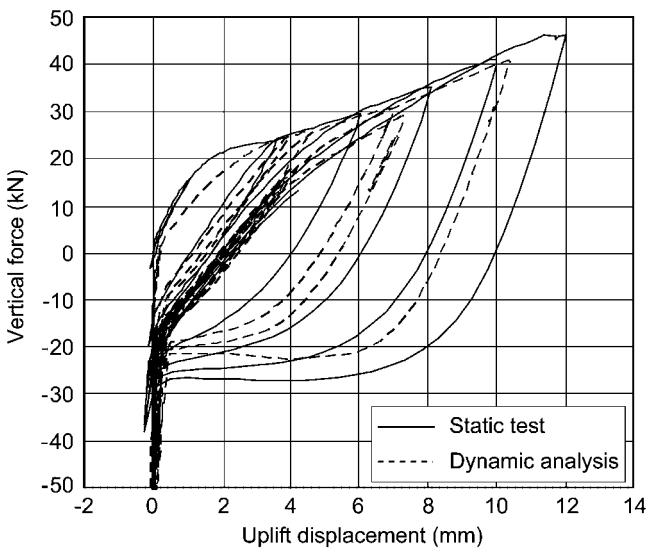

Figure 21. Vertical force versus uplift displacement at west column base of BP9-2 model. Maximum input acceleration = 5.84 m/s^2.

frame is plotted. The analytical results simulate the test results quite well. The uplift motion in the analysis occurs alternately between the west and east sides as observed in the shaking table tests. In the analysis, the maximum uplift displacement is 10.4 mm while from the test results it is 9.9 mm in the central frame and 9.7 mm in the south frame.

Figure 21 shows the relationships of the vertical force and the uplift displacement at the west column base of BP9-2 model and the test results under static loading [13]. In order to evaluate the uplift hysteretic behaviour of the yielding base plates subjected to vertical force, the static loading tests were performed after the dynamic tests using the identical base plate configuration and material prepared at the time of manufacturing the dynamic test frames. The loading history applied in static loading consisted of increasing the deformation cycles but was not based on the

DOI: 10.1002/eqe

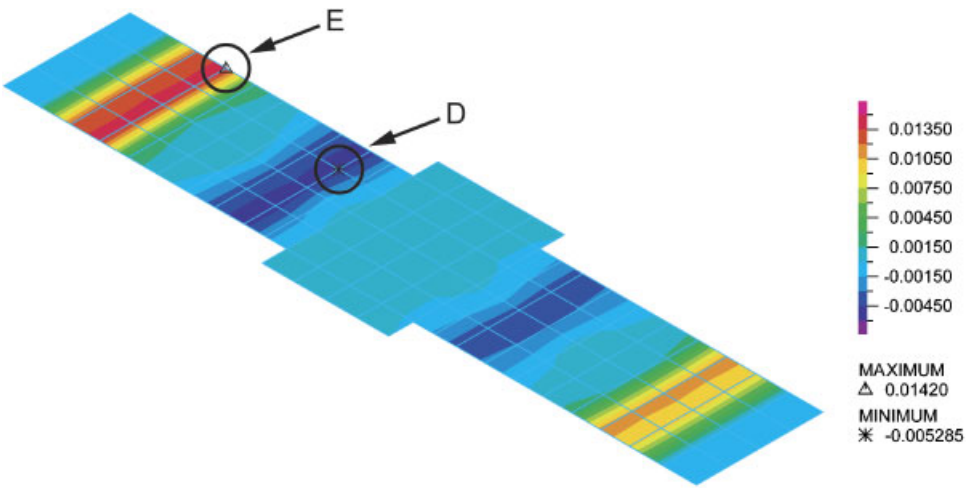

Plate 1. Strain distribution in shaking direction on bottom surface of base plate at west column base of BP9-2 model ($t = 5.05$ s).

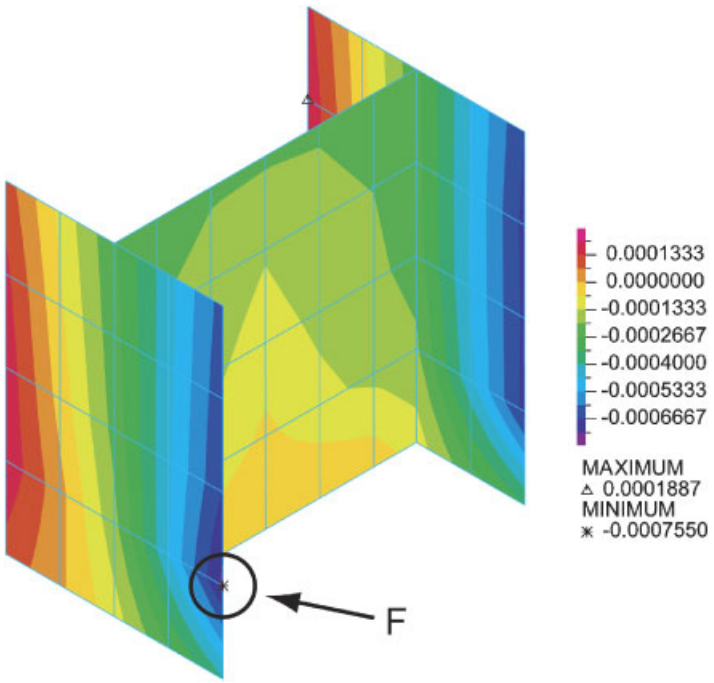

Plate 2. Strain distribution in longitudinal direction on surface at bottom of west column of BP9-2 model ($t = 5.17$ s).

DOI: 10.002/eqe

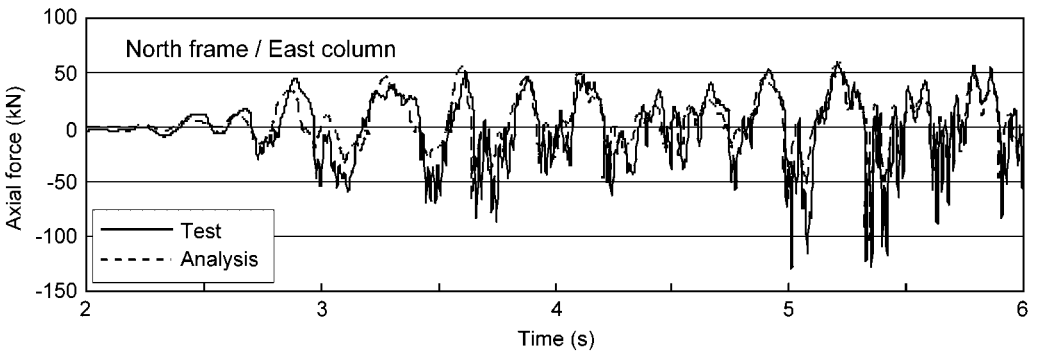

Figure 22. Time histories of axial force variations of column at first storey of BP9-2 model. Maximum input acceleration = 5.84 m/s^2.

predictions of dynamic analysis. The static test results corresponding to BP9-2 model showed that the cyclic deformation capacity was quite large, that is, the maximum uplift deformation reached more than 40 mm, a value that was four times greater than in the dynamic test. Although there is no calibration between the analytical model data and the static cyclic data, the characteristics of uplift hysteretic behaviour at the column base are correctly represented by the analysis. The energy dissipation of the yielding base plates is expected to be effective in reducing the response displacements of yielding-base-plate rocking systems.

5.2. Local behaviour and responses

Figure 22 shows the time histories of the axial force variations of the east column of the north frame at the first storey of BP9-2 model. The impact force in compression is observed approximately at the instant when the base plate touches down, although the impact effect is small as discussed in the previous section. The maximum amplitude of compressive force in the analysis is about 80% of that in the test. The reason may be that the viscous damping is assumed initial stiffness dependent in the analysis, so that the response in the higher modes such as the longitudinal vibration mode of the column is suppressed.

Plate 1 illustrates the strain distribution in the shaking direction on the bottom surface of the west base plate of BP9-2 model when the uplift displacement reaches the maximum response. The peak local strain near the column end of the base plate, at Point D in Plate 1, reaches 0.53% in compression. The maximum local strain close to the fixed nodal points of the base plate, at Point E in Plate 1, goes up to 1.42% in tension, which exceeds the yield strain of steel but is far from the fracture strain. The absolute peak strain in tension is larger than that in compression because the wing of the base plate is simultaneously subjected to bending and tension at this time.

Plate 2 illustrates the strain distribution on the surface of the bottom of the west column at the first storey, around Point C in Figure 8(a), along the axis of the member of BP9-2 model when the axial strain of the column reaches the maximum value in compression. At this time, the peak local strain in compression at Point F in Plate 1 goes up to 0.076%, which does not reach the yield strain of steel or the critical strain of the flange plate for local buckling. As a result, this confirms that local buckling never occurs in the steel plate elements of columns within the range of the maximum input accelerations in the tests.

DOI: 10.1002/eqe

6. CONCLUSIONS

The seismic response of base-plate-yielding rocking structural systems with column uplift is evaluated and compared with that of fixed-base systems by shaking table tests and numerical analyses. The studies are carried out using three-storey, 1×2 bay braced half-scale steel frames. The results of this study are summarized below.

(1) Yielding base plates both with two and four wings are feasible methods for implementing rocking structural systems with column uplift.
(2) The maximum base shears in the seismic response of the test structures with column uplift are effectively reduced in the base-plate-yielding rocking systems from those of the fixed-base system. This reduction in response for the uplifting cases is attributed to the suppression of the response deformation of the superstructure because the rocking component dominates the overall response displacement.
(3) The maximum roof displacements in the seismic response of the rocking test structures are not much different from the elastic response values of the fixed-base system. The energy dissipation of the yielding base plates is expected to be effective in reducing the response displacement of yielding-base-plate rocking systems.
(4) The maximum tensile forces at the column bases for the uplifting cases are limited to about twice the uplift yield strength of base plates after the uplift motion occurs. The increase in the tensile strength is caused by the inelastic strain hardening and large deformation effects in the wings of the base plates. The maximum compressive forces for the uplifting cases are almost the same as for the fixed base. The impact effect is small because the difference in tensile and compressive forces is primarily caused by the self-limiting tensile force in the column due to base plate yielding.
(5) The data indicate that the shear forces at the column bases of the rocking test structures are definitely transmitted through the yielding base plates during the uplift motion of the columns. It should also be noted that the uplift does not depreciate the shear capacity of the base plate in the horizontal direction.
(6) The results of the numerical simulation match the test results quite well in not only the global response, but also in the local behaviour such as the uplift displacements at the column bases and the axial forces in the columns.

The results discussed above regarding the behaviour of rocking systems are not directly relevant to the practical design of structures. Therefore, further study is needed on issues such as the effects of the vertical components of earthquake ground motions and the installation of other damper elements on rocking systems, the effect of the higher mode participation, the compatibility of vertical deflections between the rocking frame and the remainder of the building structural systems, and the actual design applications including base plate design.

ACKNOWLEDGEMENTS

This work has been stipulated by the U.S.-Japan Cooperative Structural Research Program on Smart Structural Systems (Chairpersons of the Joint Technical Coordinating Committee: Prof. S. Otani, The University of Tokyo (at that time) and Prof. M. A. Sozen, Purdue University). The authors would like to acknowledge all project members for their useful advice and suggestions. The authors express their gratitude to Ms Y. Takeuchi and Mr M. Kawakami of Kozo Keikaku Engineering Inc., and

DOI: 10.1002/eqe

Dr M. Ikarashi for their excellent support in the analytical work. The authors also express their appreciation to two anonymous reviewers for their critical comments and suggestions to improve the quality of the manuscript. Part of this work is supported by the Ministry of Education, Culture, Sports, Science and Technology (MEXT) of Japan under Grants-in-Aid for Scientific Research, Projects No. 16360284 and 16560520.

REFERENCES

1. Rutenberg A, Jennings PC, Housner GW. The response of Veterans Hospital Building 41 in the San Fernando Earthquake. *Earthquake Engineering and Structural Dynamics* 1982; **103**:359–379.
2. Hayashi Y, Tamura K, Mori M, Takahashi I. Simulation analyses of buildings damaged in the 1995 Kobe, Japan, earthquake considering soil–structure interaction. *Earthquake Engineering and Structural Dynamics* 1999; **284**:371–391.
3. Clough RW, Huckelbridge AA. Preliminary experimental study of seismic uplift of a steel frame. *Report No. UBC/EERC-77/22*, EERC, University of California, Berkeley, CA, 1977.
4. Huckelbridge AA. Earthquake simulation tests of a nine storey steel frame with columns allowed to uplift. *Report No. UBC/EERC-77/23*, EERC, University of California, Berkeley, CA, 1977.
5. Skinner RI, Robinson WH, McVerry. *An Introduction to Seismic Isolation*. Wiley: Chichester, 1993; 288–291.
6. Kasai K, Kanada M, Okuma K. Real example for a passively controlled building with stepping column: analysis and full-scale damper experiment. *Proceedings of Passive Control Symposium 2001*, Structural Engineering Research Center, Tokyo Institute of Technology, 2001; 235–249 (in Japanese).
7. Iwashita K, Kimura H, Kasuga Y, Suzuki N. Shaking table test of a steel frame allowing uplift. *Journal of Structural and Construction Engineering*, Architectural Institute of Japan, 2002; **561**:47–54 (in Japanese).
8. Meek JW. Effects of foundation tipping on dynamic response. *Journal of the Structural Division* (ASCE) 1975; **101**(ST7):1297–1311.
9. Iwashita K, Taniguchi H, Ishihara T. Energy approach to the earthquake response of building allowing uplift at pile head. *Journal of Structural and Construction Engineering* (AIJ) 2003; **564**:23–30 (in Japanese).
10. Midorikawa M, Azuhata T, Ishihara T, Wada A. Dynamic behavior of steel frames with yielding base plates in uplift motion for seismic response reduction. *Journal of Structural and Construction Engineering* (AIJ) 2003; **572**:97–104 (in Japanese).
11. Azuhata T, Midorikawa M, Ishihara T. Energy dissipation mechanism and maximum response displacement prediction of steel frames with yielding base plates in uplift motion for seismic response reduction. *Journal of Structural and Construction Engineering* (AIJ) 2004; **583**:61–68 (in Japanese).
12. ADINA R&D Inc. Theory and modelling guide—ADINA, *Report ARD 02-7*, 2002.
13. Ishihara T, Midorikawa M, Azuhata T, Wada A. Hysteresis characteristics of column base for rocking structural systems with base plate yielding. *Journal of Constructional Steel* 2003; **11**:51–56 (in Japanese).

DOI: 10.1002/eqe